Enhanced Luminance and Thermal Properties of Poly(phenylenevinylene) Copolymer Presenting Side-Chain-Tethered Silsesquioxane Units

Chia-Hung Chou, So-Lin Hsu, Siao-Wei Yeh, Hsu-Shen Wang, and Kung-Hwa Wei*

Department of Materials Science and Engineering, National Chiao Tung University, Hsinchu, Taiwan 30049, R.O.C.

Received May 24, 2005; Revised Manuscript Received August 17, 2005

ABSTRACT: We have synthesized, using the Gilch polymerization method, a new series of high-brightness, soluble copolymers (POSS-PPV-*co*-MEHPPV) of poly(*p*-phenylenevinylene) (PPV) containing side-chain-tethered polyhedral oligomeric silsesquioxane (POSS) pendent units and poly(2-methoxy-5-[2-ethylhexyloxy]-1,4-phenylenevinylene) (MEHPPV). This particular molecular architecture of POSS-PPV-*co*-MEHPPV copolymers possesses not only a larger quantum yield (0.85 vs 0.19) but also higher degradation and glass transition temperatures relative to those of pure MEHPPV. The maximum brightness of a double-layered-configured light-emitting diode (ITO/PEDOT/emissive polymer/Ca/Al) incorporating a copolymer of MEHPPV and 10 mol % PPV-POSS was 5 times as large as that of a similar light-emitting diode incorporating pure MEHPPV (2196 vs 473 cd/m^2).

Introduction

Emissive media based on electroluminescent (EL) polymers are currently under development for a number of display applications,[1−4] including large-area flat-panel displays that can be driven at low voltage. Polymer light-emitting diodes (PLEDs) are very promising candidates for the development of low-cost, multicolored, large-area flat-panel displays because their molecular structures are readily modified and because they can be handled using a range of wet processing techniques.[5,6] A number of issues remain to be resolved, however, before commercialization of these devices can occur. The formation of excimers resulting from the aggregation of their molecular chains in the solid state, and rather short operating lifetimes, owing to their low thermal stabilities. Several attempts have been made to reduce the formation of aggregates of polymer chains in the solid state. One such approach is the introduction of bulky organic units into the side chains of the polymer. This tactic has been used, for example, in the case of poly(*p*-phenylenevinylene) (PPV)-based alternating copolymers containing conjugated phenylenevinylene segments and nonconjugated spacers;[7−9] these bulky side groups disrupt the packing of the polymer chains, which results in the formation of amorphous PPVs displaying reduced aggregation. Another approach to improving the efficiency of the devices is to blend hole-transporting and electron-transporting materials to balance the injected charges.[10−12a] When such a device is operated for a long time, however, this method can cause some defect to occur in some cases.[12b−d] Other approaches include improving the antioxidative properties of the pendant groups or chain ends[13] and limiting chain mobility by blending[14] with a high-T_g polymer. One approach to not only preventing polymer chains from aggregating but also improving the antioxidative properties of their pendent groups is to use inorganic pendent groups as the side chains of the conjugated polymers.

The chemistry of polyhedral oligomeric silsesquioxane (POSS) covalently bonded to organic polymers has been developed recently. One set of members of the polyhedral oligomeric silsesquioxane family are octamers having the general formula $(RSiO_{1.5})_8$; they consist of a rigid, cubic silica core having a nanopore diameter of ca. 0.3−0.4 nm.[15] The incorporation of $(RSiO_{1.5})_8$ into some polymers leads to an enhancement of their thermal stability and mechanical properties.[16−18]

The first study in which POSS and conjugate polymers were combined involved tethering POSS to the chain ends of poly(2-methoxy-5-[2-ethylhexyloxy]-1,4-phenylenevinylene) (MEHPPV)[19] and the luminescent polymer poly(9,9′-dioctylfluorene) (PFO). The enhanced electroluminescence of these nanostructured polymers was attributed to POSS, imparting a reduction in the degree of either aggregation or excimer formation.[13] The approach of tethering POSS at the ends of a polymer's chain, however, limits the number of POSS units that can be attached. In a previous study, we synthesized a series of side-chain-tethered POSS derivatives of polyimide as a method of lowering its dielectric constant.[20] More recently, side-chain-tethered PF−POSS copolymers have been synthesized; they display a stronger and purer blue electroluminescence.[21a] In this paper, we report a new series of asymmetric PPV derivatives presenting POSS units in their side chains. We synthesized these polymers using the Gilch polymerization method. We incorporated the POSS units into the PPV to improve its thermal stability and EL characteristics. The bulky silsequioxane group was introduced at the meta position of the phenyl substitutents to inhibit intermolecular interactions between the resulting polymer chains. Such meta substitution also helps to provide an amorphous state and better processability. To the best of our knowledge, the introduction of an inorganic side group, such as POSS, into PPV-based alternating

* Corresponding author: Tel 886-35-731871, Fax 886-35-724727, e-mail khwei@cc.nctu.edu.tw.

10.1021/ma051055u CCC: $30.25
Published on Web 10/07/2005

Scheme 1.[a] **Synthesis of POSS-PPV-*co*-MEHPPV Copolymers**

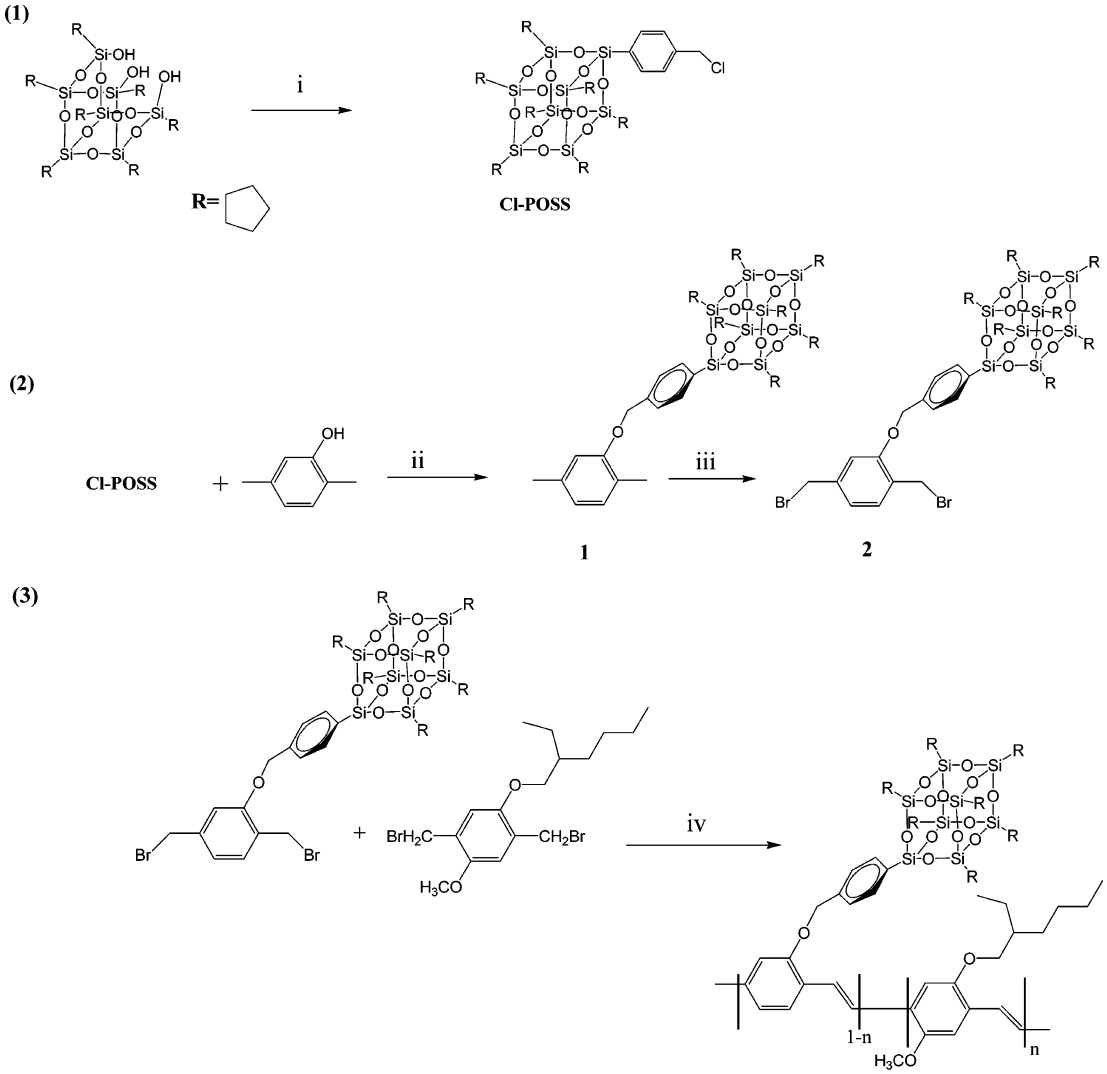

[a] Reagents and conditions: i, trichloro[4-(chloromethyl)phenyl]silane, $HNEt_3Cl$; ii, K_2CO_3, DMF/THF; iii, *N*-bromosuccinimide (NBS)/AIBN/CCl_4; iv, *tert*-BuOK/THF.

copolymers has not yet been described. We believe that developing POSS/poly(*p*-phenylenevinylene) copolymers having well-defined architectures will allow its luminescence properties to be tailored more precisely through modifications of its molecular structure.

Experimental Section

Chlorobenzylcyclopentyl-POSS[19a] was synthesized according to literature procedures. THF was distilled under nitrogen from sodium benzophenone ketyl; other solvents were dried using standard procedures. All other reagents were used as received from commercial sources, unless otherwise stated.

Chlorobenzylcyclopentyl-POSS. ^{1}H NMR (300 MHz, $CDCl_3$): δ 7.64 (d, J = 8.1 Hz, 2H), 7.37 (d, J = 8.1 Hz, 2H), 4.57 (s, 2H), 2.26−1.21 (m, 56H), 1.16−0.81 ppm (m, 7H). ^{29}Si NMR (600 MHz, THF): −67.8, −68.2, −79.6 ppm.

Synthesis of POSS-CH_3 (1). 2,5-Dimethylphenol (238 mg, 1.95 mmol) was stirred with K_2CO_3 (4.58 g, 33.18 mmol) and KI (1.57 g, 9.48 mmol) in DMF (30 mL) and THF (15 mL) at room temperature for 1 h. A small amount of Cl-POSS (2.0 g, 1.95 mmol) was added, and then the whole mixture was heated at 70 °C for 3 h. The reaction mixture was then slowly poured into water (300 mL) and extracted with chloroform (3 × 50 mL). The combined extracts were dried ($MgSO_4$), the solvents were evaporated, and the residue was purified by column chromatography (hexane/chloroform, 1:10) to afford **1** (1.86 g, 81%). ^{1}H NMR (300 MHz, $CDCl_3$): δ 7.70 (d, J = 8.1 Hz, 2H), 7.51−7.31 (b, 3H), 7.03 (d, J = 6.9 Hz, 1H), 6.67 (s, 1H), 5.09 (s, 2H), 2.37 (s, 3H), 2.32 (s, 3H), 2.27−1.21 (m, 56H), 1.17−0.81 ppm (m, 7H).

Synthesis of POSS-CH_2Br (2). A mixture of POSS-CH_3 (**1**; 600 mg, 0.510 mmol), NBS (198.6 mg, 1.02 mmol), and AIBN (8.0 mg) was heated under reflux in carbon tetrachloride under nitrogen for 3 h. The reaction mixture was filtered to remove succinimide, the solvent was evaporated, and the residue was purified by column chromatography (hexane/chloroform, 1:10). ^{1}H NMR (300 MHz, $CDCl_3$) δ: 7.73 (d, J = 8.1 Hz, 2H), 7.59 (d, J = 6.9 Hz, 1H), 7.38 (d, J = 8.1 Hz, 2H), 7.09 (d, J = 6.9 Hz, 1H), 7.01 (s, 1H), 5.18 (s, 2H), 4.73 (s, 2H), 4.57 (s, 2H), 2.26−1.21 (m, 56H), 1.16−0.81 ppm (m, 7H). Anal. Calcd for $C_{50}H_{76}Br_2O_{13}Si_8$ (%): C, 47.30; H, 6.03. Found: C, 47.18; H, 6.09.

General Procedure for the Synthesis of Copolymers POSS−PPV-*co*-MEHPPV. A solution of potassium *tert*-butoxide (1 M in THF) was added to a solution of the monomer in dry THF, and then the mixture was stirred for 4 h. End-group capping was performed by heating the solution under reflux for 1 h in the presence of tetrabutylbenzyl bromide. Addition of the THF solution to methanol precipitated the polymer, which was collected, washed with methanol, and stirred in a mixture of methanol and water (1:1) for 1 h. The polymer was collected, washed with methanol, filtered, and dried at 50 °C for 24 h. After cooling, the polymer was recovered by precipitating it into a mixture of methanol and acetone (4:1). The crude polymer was collected, purified twice

Table 1. Physical Properties of the POSS-PPV-*co*-MEHPPV Copolymers

	T_g (°C)	T_d[a] (°C)	M_n	M_w	PDI	yield (%)
MEHPPV	71	370	61 000	111 000	1.82	78
POSS-PPV1-*co*-MEHPPV	90	381	55 000	107 000	1.95	66
POSS-PPV3-*co*-MEHPPV	96	395	52 000	98 000	1.88	64
POSS-PPV5-*co*-MEHPPV	*b*	417	48 000	91 000	1.90	69
POSS-PPV10-*co*-MEHPPV	*b*	453	39 000	73 000	1.87	60

[a] Temperature at which 5% weight loss occurred, based on the initial weight. [b] The glass transition disappeared because of the steric hindrance imposed on the main molecular chains by the POSS units.

by reprecipitation from THF into methanol, and subsequently dried under vacuum at 50 °C for 24 h. The ^{1}H and ^{13}C NMR spectra of MEHPPV and PPV−POSS appear to be identical because of the low content of POSS in the latter polymer.

Characterization. ^{1}H, ^{13}C, and ^{29}Si nuclear magnetic resonance (NMR) spectra of the compounds were obtained using a Bruker DRX 300 MHz spectrometer. Mass spectra of the samples were obtained on a JEOL JMS-SX 102A spectrometer. Fourier transform infrared (FTIR) spectra of the synthesized materials were acquired using a Nicolet 360 FT-IR spectrometer. Gel permeation chromatographic analyses were performed on a Waters 410 differential refractometer and a Waters 600 controller (Waters styragel column). All GPC analyses of polymers in THF solutions were performed at a flow rate of 1 mL/min at 40 °C; the samples were calibrated using polystyrene standards. Thermogravimetric analysis (TGA) and differential scanning calorimetry (DSC) measurements were performed under a nitrogen atmosphere at heating rates of 20 and 10 °C/min, respectively, using Du Pont TGA-2950 and TA-2000 instruments, respectively. UV−vis absorption and photoluminescence (PL) spectra were recorded on a HP 8453 spectrophotometer and a Hitachi F-4500 luminescence spectrometer, respectively. Before investigating the thermal stability of the synthesized polymers, their polymer films were annealed in air at 200 °C for 2 h.

Device Fabrication and Testing. The electroluminescent (EL) devices were fabricated on an ITO-coated glass substrate that was precleaned and then treated with oxygen plasma before use. A layer of poly(ethylenedioxythiophene):poly(styrenesulfonate) (PEDOT:PSS, Baytron P from Bayer Co.; ca. 40 nm thick) was formed by spin-coating it from an aqueous solution (1.3 wt %). The EL layer was spin-coated, at 1500 rpm from the corresponding toluene solution (15 mg mL^{-1}), on top of the vacuum-dried PEDOT:PSS layer. The nominal thickness of the EL layer was 65 nm. Using a base pressure below 1×10^{-6} Torr, a layer of Ca (35 nm) was vacuum-deposited as the cathode, and a thick layer of Al was deposited subsequently as the protecting layer. The current−voltage characteristics were measured using a Hewlett-Packard 4155B semiconductor parameter analyzer. The power of the EL emission was measured using a Newport 2835-C multifunction optical meter. The brightness was calculated using the forward output power and the EL spectra of the devices; a Lambertian distribution of the EL emission was assumed.

Results and Discussion

Figure 1 displays the ^{1}H NMR spectra of Cl-POSS, POSS-CH_3 (**1**), and POSS-CH_2Br (**2**). The CH_2 peak of Cl-POSS (4.47 ppm) shifted downfield to 5.14 ppm in POSS-CH_3. The ratio of the peak areas of the benzylic CH_2 and CH_2Br protons is ca. 1:2. Taken together, these data suggest that Cl-POSS had reacted with 2,5-dimethylphenol to form POSS-CH_3. Table 1 lists the thermal properties and molecular weight distributions of the POSS-PPV-*co*-MEHPPV copolymers. Both the thermal degradation and glass transition temperatures increased substantially as the amount of POSS in MEHPPV increased, particularly for the case where 10 mol % POSS was tethered to MEHPPV: we observed an 83 °C increase in the value of T_d and a disappearance of any glass transition.[21b] This situation arose because

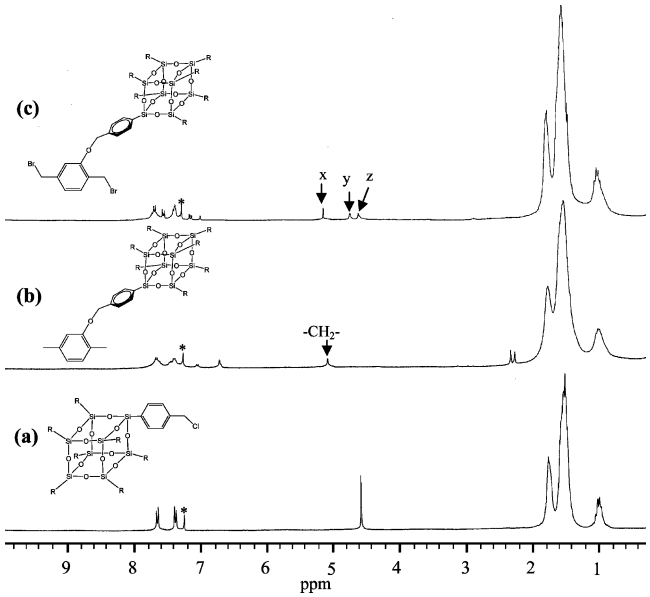

Figure 1. ^{1}H NMR spectra of (a) Cl-POSS, (b) POSS-CH_3, and (c) POSS-CH_2Br.

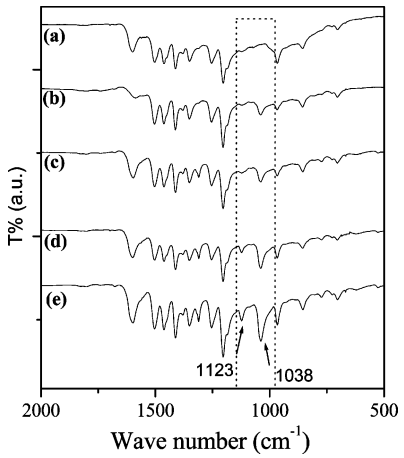

Figure 2. FTIR spectra of (a) MEHPPV, (b) POSS-PPV1-*co*-MEHPPV, (c) POSS-PPV3-*co*-MEHPPV, (d) POSS-PPV5-*co*-MEHPPV, and (e) POSS-PPV10-*co*-MEHPPV.

the tethered bulky POSS enhanced the thermal stability and retarded the mobility of the polymer main chain. The molecular weights of the POSS-PPV-*co*-MEHPPV copolymers decreased upon increasing the POSS content; this phenomenon can be attributed to the steric hindrance caused by the POSS units during the polymerization process. Figure 2 displays FTIR spectra of MEHPPV copolymers containing different amounts of POSS. The FTIR spectrum of POSS displays two major characteristic peaks: the Si−C band at 1038 cm^{-1} and the Si−O−Si band at 1123 cm^{-1}.

Table 2 lists the wavelengths of the absorption, the location of the PL maxima, and the quantum yields of POSS-PPV-*co*-MEHPPV. The absorption and emission

Table 2. Optical Properties of the POSS-PPV-*co*-MEHPPV Nanocomposites

	λ_{max} (UV, nm)		λ_{max} (PL, nm)[a]		QY
	solution[b]	film	solution[b]	film	film[c]
MEHPPV	499	517	553 (592)	591 (634)	0.19
POSS-PPV1-*co*-MEHPPV	499	512	552 (591)	588 (633)	0.43
POSS-PPV3-*co*-MEHPPV	498	512	552 (591)	586 (632)	0.62
POSS-PPV5-*co*-MEHPPV	497	511	552 (591)	585 (631)	0.84
POSS-PPV10-*co*-MEHPPV	494	505	551 (590)	584 (631)	0.87

[a] The data in parentheses are the wavelengths of the shoulders and subpeaks. [b] The absorption and emission were measured in THF. [c] PL quantum yield estimated relative to a sample of Rhodamine 6G ($\Phi_r = 0.95$).[23−25]

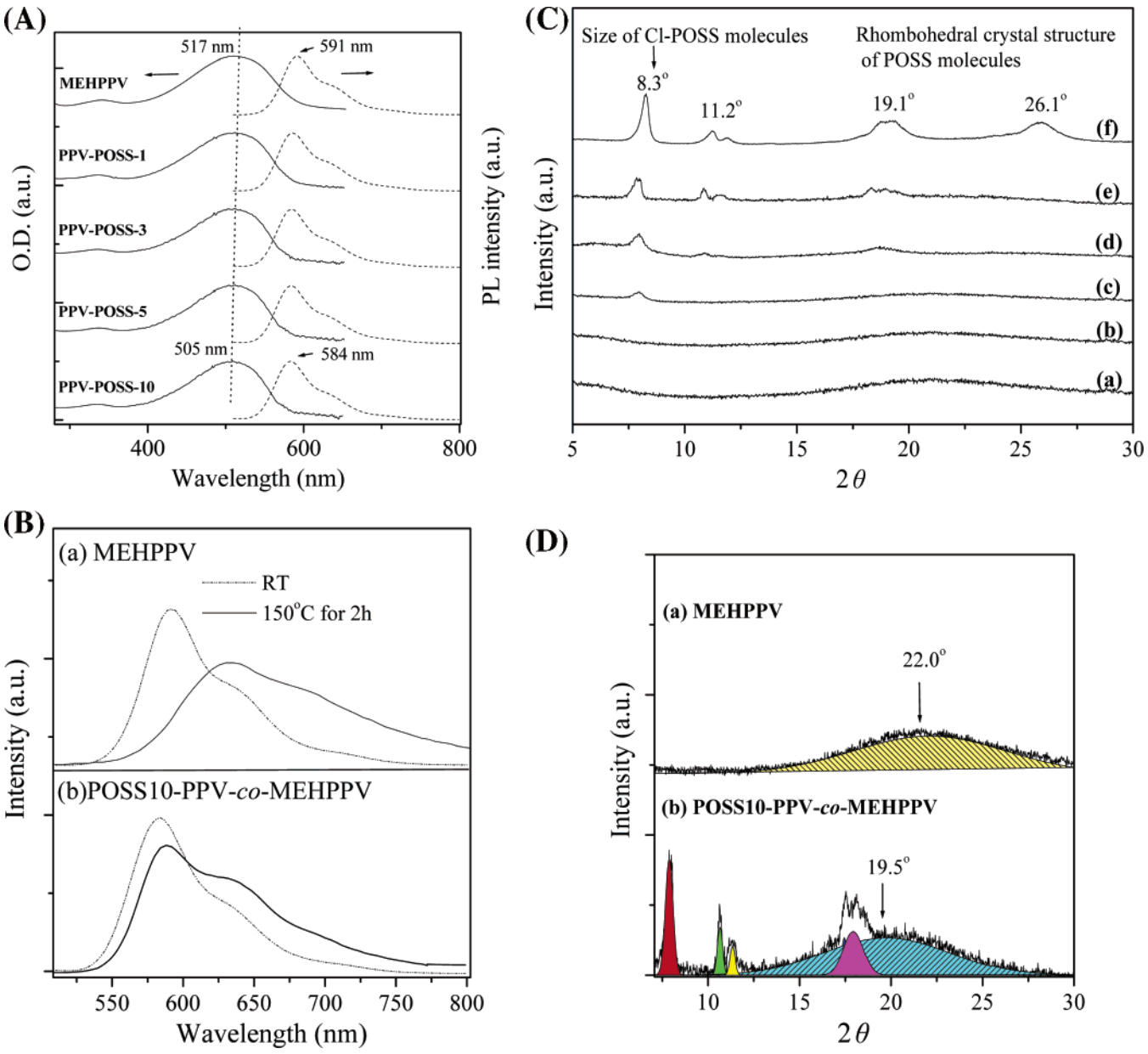

Figure 3. (A) UV−vis absorption and PL spectra of (a) MEHPPV, (b) POSS-PPV1-*co*-MEHPPV, (c) POSS-PPV3-*co*-MEHPPV, (d) POSS-PPV5-*co*-MEHPPV, and (e) POSS-PPV10-*co*-MEHPPV recorded in the solid state. (B) Normalized (relative to their maximum wavelengths) PL spectra of (a) MEHPPV and (b) POSS-PPV10-*co*-MEHPPV annealed at room temperature and 150 °C in the solid state. (C) X-ray diffraction spectra of (a) MEHPPV, (b) POSS-PPV1-*co*-MEHPPV, (c) POSS-PPV3-*co*-MEHPPV, (d) POSS-PPV5-*co*-MEHPPV, (e) POSS-PPV10-*co*-MEHPPV, and (f) Cl-POSS. (D) Deconvoluted X-ray diffraction spectra of (a) MEHPPV and (b) POSS-PPV10-*co*-MEHPPV.

peak maxima of MEHPPV occurred at 499 and 553 nm, respectively; these values are close to those reported in the literature.[19] We observed no aggregation band in these spectra because THF is a good solvent for MEH-PPV. The absorption and emission peaks for MEHPPV and POSS-PPV-*co*-MEHPPV are almost identical. For each polymer, the absorption peak maximum in solution (THF) is located between 499 and 494 nm, with a slight blue shift caused by the presence of POSS; the PL maxima occur at similar wavelengths for all of the polymers. Figure 3A presents the normalized absorption and PL emission spectra of the MEHPPV−POSS co-

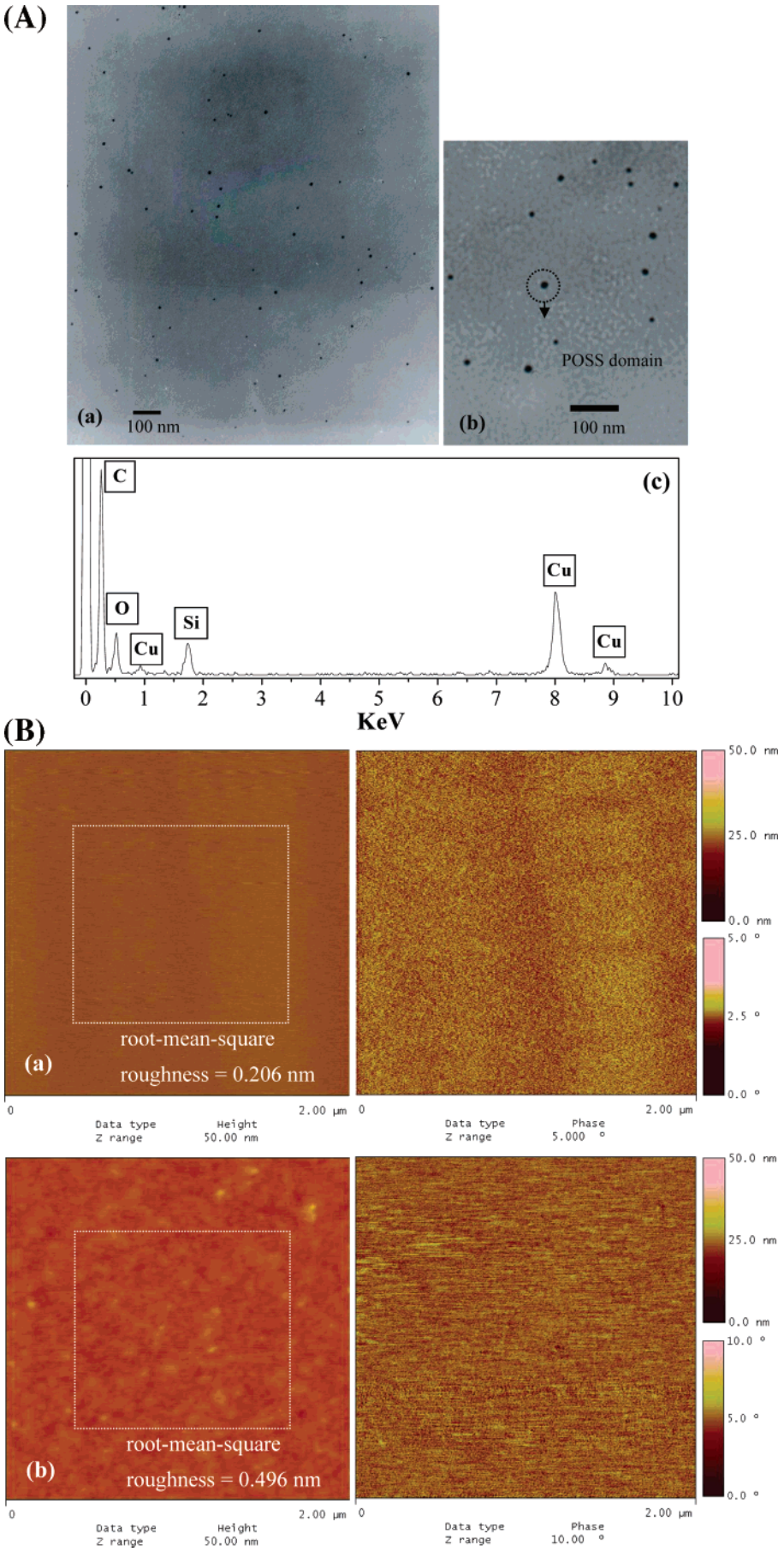

Figure 4. (A) (a) Transmission electron micrograph of POSS-PPV10-*co*-MEHPPV; (b) enlarged view; (c) EDS of POSS-PPV10-*co*-MEHPPV. (B) Surface roughness of thin films of (a) MEHPPV and (b) POSS-PPV10-*co*-MEHPPV.

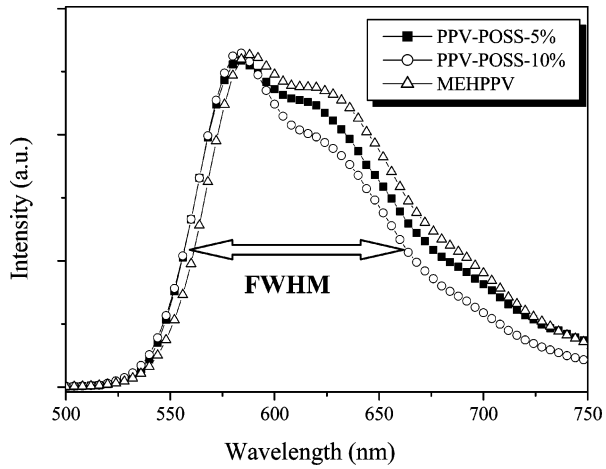

Figure 5. Electroluminescence spectra of the devices prepared from POSS-PPV-*co*-MEHPPV in the configuration ITO/PEDOT/polymer/Ca/Al.

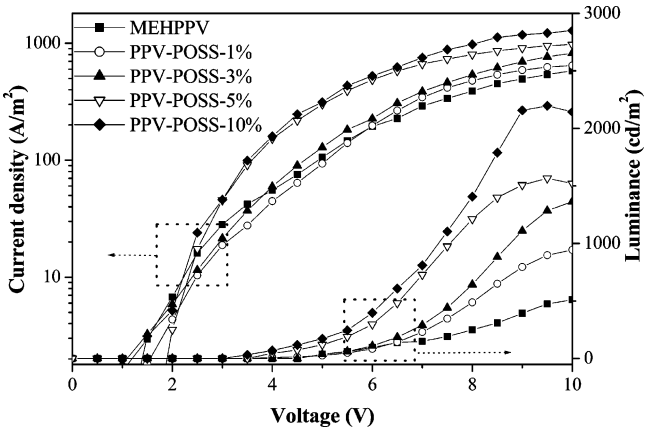

Figure 6. *I*−*L*−*V* curves of the devices prepared from POSS-PPV-*co*-MEHPPV and MEHPPV in the configuration ITO/PEDOT/polymer/Ca/Al.

polymer films. The quantum yields of the POSS-PPV-*co*-MEHPPV copolymers increased substantially as the amount of tethered POSS increased.[30] In particular, the quantum yield of MEHPPV containing 10% POSS was 4 times higher than that of pure MEHPPV (0.87 vs 0.19). We attribute this finding to the steric hindrance caused by the POSS units in preventing aggregation of the PPV main chains, which, in turn, reduces the degree of dimer formation after excitation. This improved quantum yield, which has not been reported in any previous studies of POSS/PPV copolymers, is a direct result of employing this particular side-chain-tethered POSS architecture.

For fresh MEH-PPV film, the yellowish peak at ~590 nm originates from single chain exciton emissions,[26] whereas the reddish peak at 630 nm is related to emissions from interchain species, such as aggregates or excimers.[26a] The difference in the PL spectra of the fresh MEH-PPV and POSSPPV-*co*-MEHPPV film is small because both polymer chains have not reached equilibrium states by their preparation process (i.e., spin-coating). By annealing the polymer films at higher temperatures as in the work by Schwartz[27] and Yang Yang[28] et al., one could see some more profound changes in their PL spectra. For instance, Figure 3B shows that after annealing MEHPPV film at 150 °C for 2 h under air its PL spectrum displays a red-shifted broad main peak at 630 nm, indicating formation of aggregates. While the main emission peak for annealed POSS-PPV10-*co*-MEHPPV film remain near 590 nm, with a weak peak at 630 nm. Therefore, at the equilibrium states, there is a distinct difference in their PL spectra, due to the bulky and rigid POSS groups tethered to the side of MEHPPV chains. The same phenomena are also observed in EL spectra (Figure 5).

We have carried out X-ray diffraction studies for confirming that interchain distance of PPV was increased by side-chain-tethered POSS. Figure 3C displays the X-ray diffraction curves of Cl-POSS, MEHPPV, and PPV-POSS. There are three distinct diffraction peaks at $2\theta = 8.3°$, 19.1°, and 26.1° for Cl-POSS (Figure 3f), which correspond to *d*-spacings of 10.5, 4.6, and 3.3 Å, respectively. The *d*-spacing of 10.5 Å reflects the size of the Cl-POSS molecules; the other two spacings are owing to the rhombohedral crystal structure of POSS molecules.[29a] For pure MEHPPV and PPV−POSS copolymers, it is evident that they are amorphous and have no side chain alignment. The nearly amorphous structure of pure MEHPPV (Figure 3C-a) originates from the two highly asymmetric substituents: the methoxy and 2-methoxy 5-(2′-ethoxyhexyloxy) for MEH-PPV.[29b] When POSS molecules were tethered to PPV, the average interchain distance increased appreciably from X-ray diffraction results. For instance, in the presence of 10% POSS (PPV-POSS-10%), the interchain distance increases to 4.6 Å (19.5°) from 4.0 Å (22.0°) for MEHPPV after deconvolution of the X-ray diffraction curve.

Figure 4A presents a transmission electron microscopy (TEM) image of our POSS-PPV10-*co*-MEHPPV sample.[31] This image reveals that no large aggregates were formed, but small domains of POSS are present; these POSS domains are dispersed evenly in the polymer matrix—a situation that we confirmed by analyzing this sample's energy dispersive spectrum (EDS; Figure 4A-c). The topology of POSS-PPV-*co*-MEHPPV copolymers films were studied with atomic force microscopy (AFM). Figure 4B shows the height image and the phase image of MEH-PPV and POSS-PPV10-*co*-MEHPPV polymer films prepared with chlorobenzene as the solvent. The surface roughness of PPV-POSS film is larger than that of pure MEHPPV (0.496 nm vs 0.206 nm) due to the presence of POSS. The phase images also show that POSS groups are dispersed homogeneously in the whole system.

Electroluminescence Characteristics. Figure 5 displays the electroluminescence (EL) spectra of POSS-PPV-*co*-MEHPPV devices. The EL device prepared from MEHPPV emits a strong peak at 590 nm and a vibronic signal in the range 610−620 nm, which is due presumably to the aggregation of MEHPPV and its excimer formation, as discussed earlier. The introduction of bulky siloxane units into the PPV side chains presumably increases the interchain distance, thereby retarding interchain interactions and leading to a reduction in the degree of exciton migration to defect sites.[22] Figure 6 displays the variations in the current density and brightness of the EL devices. The turn-on voltage decreased to 2.5 V for PPV containing 10% POSS from 3.5 V for the pure-MEHPPV EL device. As indicated in Figure 6, a more than 4-fold increase in the maximum brightness of the POSS-PPV10-*co*-MEHPPV device occurs with respect to that of the pure-MEHPPV EL device (2196 vs 473 cd/m^2) at a driving voltage of 9.5 V. The efficiency of POSS-PPV10-*co*-MEHPPV is 1.83 cd/A at a current density of 1221 A/m^2.

These improvements might be due to a decreased degree of aggregation upon the incorporation of the POSS units into the PPV chains.

Summary

We have synthesized a novel poly(*p*-phenylenevinylene) side-chain-tethered polyhedral silsesquioxane (POSS-PPV-*co*-MEHPPV) that possesses a well-defined architecture. This particular molecular architecture of PPV-POSS increases the quantum yield of MEHPPV significantly by reducing the degree of interchain aggregation; it also results in a much brighter red light from the EL device by decreasing the degree of aggregation between the polymer chains.

Acknowledgment. We acknowledge Chunghwa Picture Tubes, Ltd., and the National Science Council, Taiwan, for funding this work through Grant NSC 94-2120-M-009-001. Mr. Chen-Ping Chen and Mr. Yao-Te Chang are also acknowledged for experimental assistance and helpful discussions.

Supporting Information Available: Normalized UV–vis absorption and photoluminescence spectra and DSC and TGA traces of MEHPPV and PPV-POSS. This material is available free of charge via the Internet at http://pubs.acs.org.

References and Notes

(1) Ranger, M.; Rondeau, D.; Leclerc, M. *Macromolecules* **1997**, *30*, 7686.
(2) Yu, W.-L.; Pei, J.; Cao, Y.; Huang, W.; Heeger, A. J. *Chem. Commun.* **1999**, 1837.
(3) Pei, J.; Yu, W.-L.; Huang, W.; Heeger, A. J. *Chem. Commun.* **2000**, 1631.
(4) Ego, C.; Marsitzky, D.; Becker, S.; Zhang, J.; Grimsdale, A. C.; Müllen, K.; MacKenzie, J. D.; Silva, C.; Friend, R. H. *J. Am. Chem. Soc.* **2003**, *125*, 437.
(5) Mitschke, U.; Baüerle, P. *J. Mater. Chem.* **2000**, *10*, 1471.
(6) Kraft, A.; Grimsdale, C.; Holmes, A. B. *Angew. Chem., Int. Ed.* **1998**, *37*, 402.
(7) (a) Sokolik, I.; Yang, Z.; Karasz, F. E.; Morton, D. C. *J. Appl. Phys.* **1993**, *74*, 3584. (b) Hsieh, B. R.; Yu, Y.; Forsythe, E. W.; Schaaf, G. M.; Feld, W. A. *J. Am. Chem. Soc.* **1998**, 231. (c) Johansson, D. M.; Srdanov, G.; Yu, G.; Theander, M.; Inganas, O.; Andersson, M. R. *Macromolecules* **2000**, *33*, 2525.
(8) (a) Yang, Z.; Karasz, F. E.; Geise, H. J. *Macromolecules* **1993**, *26*, 6570. (b) Spreitzer, H.; Becker, H.; Kluge, E.; Kreuder, W.; Schenk, H.; Demandt, R.; Schoo, H. *Adv. Mater.* **1998**, *10*, 1340. (c) Ahn, T.; Jang, M. S.; Shim, H.-K.; Hwang, D.-H.; Zyung, T. *Macromolecules* **1999**, *32*, 3279. (d) Becker, H.; Spreitzer, H.; Ibrom, K.; Kreuder, W. *Macromolecules* **1999**, *32*, 4925. (e) Becker, H.; Spreitzer, H.; Kreuder, W.; Kluge, E.; Schenk, H.; Parker, I.; Cao, Y. *Adv. Mater.* **2000**, *12*, 42.
(9) (a) Pasco, S. T.; Lahti, P. M.; Karasz, F. E. *Macromolecules* **1999**, *32*, 6933. (b) Chen, Z. K.; Lee, N. H. S.; Wei, H.; Xu, Y. S.; Cao, Y. *Macromolecules* **2003**, *36*, 1009.
(10) Jin, S. H.; Jung, J. E.; Park, D. K.; Jeon, B. C.; Kwon, S. K.; Kim, Y. H.; Moon, D. K.; Gal, Y. S. *Eur. Polym. J.* **2001**, *37*, 921.
(11) Lee, S. H.; Jin, S. H.; Moon, S. B.; Song, I. S.; Kim, W. H.; Kwon, S. K.; Park, N. K.; Han, E. M. *Mol. Cryst. Liq. Cryst.* **2000**, *349*, 507.
(12) (a) Jin, S. H.; Kim, W. H.; Song, I. S.; Kwon, S. K.; Lee, K. S.; Han, E. M. *Thin Solid Films* **2000**, *363*, 255. (b) Huber, J.; Mullen, K.; Salbeck, J.; Schenk, H.; Scherf, U.; Stehlin, T.; Stern, R. *Acta Polym.* **1994**, *45*, 244. (c) Lemmer, U.; Heun, S.; Mahrt, R. F.; Scherf, U.; Hopmeier, M.; Sieger, U.; Gobel, E. O.; Mullen, K.; Bassler, H. *Chem. Phys. Lett.* **1995**, *240*, 373. (d) Grell, M.; Bradley, D. D. C.; Ungar, G.; Hill, J.; Whitehead, K. S. *Macromolecules* **1999**, *32*, 5810.
(13) (a) Xiao, S.; Nguyen, M.; Gong, X.; Cao, Y.; Wu, H.; Moses, D.; Heeger, A. J. *Adv. Funct. Mater.* **2003**, *13*, 25. (b) Lin, W. J.; Chen, W. C.; Wu, W. C.; Niu, Y. H.; Jen, A. K. Y. *Macromolecules* **2004**, *37*, 2335. (c) Lee, J.; Cho, H.-J.; Jung, B.-J.; Cho, N. S.; Shim, H.-K. *Macromolecules* **2004**, *37*, 8523.
(14) Kulkarni, A. P.; Jenekhe, S. A. *Macromolecules* **2003**, *36*, 5285.
(15) Zhang, C.; Babonneau, F.; Bonhomme, C.; Laine, R. M.; Soles, C. L.; Hristov, H. A.; Yee, A. F. *J. Am. Chem. Soc.* **1998**, *120*, 8380.
(16) Lichtenhan, J. D.; Vu, N. Q.; Carter, J. A.; Gilman, J. W.; Feher, F. J. *Macromolecules* **1993**, *26*, 2141.
(17) Lichtenhan, J. D.; Otonari, Y. A.; Carr, M. J. *Macromlecules* **1995**, *28*, 8435.
(18) Feher, F. J.; Soulivong, D.; Eklud, A. G.; Wyndham, K. D. *Chem. Commun.* **1997**, 1185.
(19) (a) Gustafsson, G.; Cao, Y.; Treacy, G. M.; Klavetter, F.; Colaneri, N.; Heeger, A. J. *Nature (London)* **1992**, *357*, 477. (b) Aratani, S.; Zhang, C.; Pakbaz, K.; Hoger, S.; Wudl, F.; Heeger, A. J. *J. Electron. Mater.* **1993**, *22*, 745. (c) Yang, Y.; Heeger, A. J. *Appl. Phys. Lett.* **1994**, *64*, 1245. (d) Braun, D.; Heeger, A. J. *Appl. Phys. Lett.* **1991**, *58*, 1982.
(20) (a) Leu, C. M.; Reddy, G. M.; Wei, K. H.; Shu, C. F. *Chem. Mater.* **2003**, *15*, 2261. (b) Leu, C. M.; Chang, Y. T.; Wei, K. H. *Chem. Mater.* **2003**, *15*, 3721. (c) Leu, C. M.; Chang, Y. T.; Wei, K. H. *Macromolecules* **2003**, *36*, 9122.
(21) (a) Chou, C.-H.; Hsu, S.-L.; Dinakaran, K.; Chiu, M.-Y.; Wei, K.-H. *Macromolecules* **2005**, *38*, 745. (b) Chen, S. H.; Su, A. C.; Chou, H. L.; Peng, K. Y.; Chen, S. A. *Macromolecules* **2004**, *37*, 167.
(22) Grimsdale, A. C.; Leclère, P.; Lazzaroni, R.; MacKenzie, J. D.; Murphy, C.; Setayesh, S.; Silva, C.; Friend, R. H.; Müllen, K. *Adv. Funct. Mater.* **2002**, *12*, 729.
(23) Kurian, A.; George, N. A.; Paul, B.; Nampoori, V. P. N.; Vallabhan, C. P. G. *Laser Chem.* **2002**, *20*, 99.
(24) Heldt, J. R.; Heldt, J.; Obarowska, M.; Mielewska, B.; Kamiński, J. *J. Fluoresc.* **2002**, *11*, 335.
(25) Magde, D.; Wong, R.; Seybold, P. G. *Photochem. Photobiol.* **2002**, *75*, 327.
(26) (a) Shi, Y.; Liu, J.; Yang, Y. *J. Appl. Phys.* **2000**, *87*, 4254. (b) Nguyen, T.-Q.; Martini, I.; Liu, J.; Schwartz, B. J. *J. Phys. Chem. B* **2000**, *104*, 237. (c) Nguyen, T.-Q.; Doan, V.; Schwartz, B. J. *J. Chem. Phys.* **1999**, *110*, 4068.
(27) (a) Nguyen, T.-Q.; Schwartz, B. J.; Schaller, R. D.; Johnson, J. C.; Lee, L. F.; Haber, L. H.; Saykally, R. J. *J. Phys. Chem. B* **2001**, *105*, 5153. (b) Nguyen, T.-Q.; Schwartz, B. J. *J. Chem. Phys.* **2002**, *116*, 8198.
(28) (a) Liu, J.; Shi, Y.; Yang, Y. *Adv. Funct. Mater.* **2001**, *11*, 420. (b) Shi, Y.; Liu, J.; Yang, Y. *J. Appl. Phys.* **2000**, *87*, 4254.
(29) (a) Zheng, L.; Waddon, A. J.; Farris, R. J.; Coughlin, E. B. *Macromolecules* **2002**, *35*, 2375. (b) Tretiak, S.; Saxena, A.; Martin, R. L.; Bishop, A. R. *J. Phys. Chem. B* **2000**, *104*, 7029.
(30) (a) PL quantum yield (Φ_{FL}) was determined by using Rhodamine 6G ($\Phi_r = 0.95$) as a reference that is dispersed in poly(methyl methacrylate) (PMMA) at low concentration (10^{-3} M) with the film thickness being 100 ± 10 nm. The quantum yield of a sample, Φ_s, can be calculated by the following equation: $\Phi_s = (A_r/A_s)(F_s/F_r)\Phi_r$, where A_s and A_r are the respective optical density of the sample and the reference at their excitation wavelengths and F_r and F_s are the corresponding areas under their emission peaks. (b) Kang, B. S.; Kim, D. H.; Lim, S. M.; Kim, J.; Seo, M.-L.; Bark, K.-M.; Shin, S. C.; Nahm, K. *Macromolecules* **1997**, *30*, 7196.
(31) Transmission electron microscopy was performed on a Hitachi H-600 instrument operated at 100 kV and on a JEOL-2010 TEM operated at 200 kV at the Center for Nano Science & Technology (CNST). The ultrathin sections of POSS-PPV-*co*-MEHPPV copolymer prepared for TEM studies were microtomed using a Leica Ultracut Uct apparatus equipped with a diamond knife and subsequently deposited on copper grids. The microtomed thin films, corresponding to the section of the POSS-PPV-*co*-MEHPPV copolymer, were also observed using a Digital Nanoscope IIIa atomic force microscope (AFM).

MA051055U